temperature dependent shows that the coupling between the spins is not complete, so that in order to describe the lowest energy levels of $CoBr_2(DTBNO)_2$ the exchange spin Hamiltonian[17] can be used

$$H = J(S_1 \cdot S_2 + S_2 \cdot S_3) + J' S_1 \cdot S_3 \quad (1)$$

where 1 and 3 refer to the two nitroxide spins, $S_1 = S_3 = {}^1/_2$, and 2 to the cobalt center, $S_2 = {}^3/_2$. Coupling the three spins yields one sextet, two quartets, and one doublet state, whose energies are given in Table I.

It is apparent that the spin doublet is the ground state if $J$ is positive and $J'$ negative or, when both $J$ and $J'$ are positive, if $J > {}^2/_5 J'$. Despite the fact that the magnetic susceptibilities are affected by an error, it may be concluded, with use of the high-temperature data of Beck et al.[13] and our liquid-helium data, that $J$ must be antiferromagnetic and must be larger than 200 $cm^{-1}$, showing that the metal and ligand spins must be fairly substantially coupled in this pseudotetrahedral complex. $J'$ remains largely undetermined.

The experimental $g$ values show large deviations from the free-electron value, which at first glance are surprising. However, they can be easily rationalized by using the relations of Table I, which relate the $g$ values of the individual spins and those of the coupled system. These relations were obtained according to an extension of the procedures normally used for calculating the $g$ values of pairs.[17-19] In fact the two spins $S_1$ and $S_3$ may be coupled first to give an intermediate spin $S'$ to which the usual formulas to calculate $g$ can be applied. Then $S'$ is coupled to $S_2$, again with the $g$ values calculated in the coupled representation $S$.

The free radical can be reasonably assumed to have an isotropic g tensor, $g_{1/2} = 2.00$. With use of the relations of Table I, the $g$ value of the cobalt ion is not known, but for the radical the values of $g_{3/2}$ can be calculated from the experimental data as $g_{1,3/2} = 2.17$, $g_{2,3/2} = 2.30$, and $g_{3,3/2} = 2.41$. These values compare favorably with those previously reported for the pseudotetrahedral complex $CoCl_2(Ph_3PO)_2$: $g_\parallel = 2,31$, $g_\perp = 2.35$. The orthorhombic symmetry of the $g$ values of the $CoBr_2(DTBNO)_2$ complex may reflect a more distorted coordination environment for the latter. On the other hand, the high sensitivity of the $g$ values of high-spin cobalt(II) to distortions in the coordination sphere are now well-known.[16]

In conclusion low-temperature magnetic susceptibility and EPR data show that the ground state of $CoBr_2(DTNBO)_2$ is a spin doublet originating from the antiferromagnetic coupling between the cobalt and free-radical magnetic orbitals.

**Acknowledgment.** Thanks are due to Professor A. Vacca, ISSECC, CNR, for allowing us to record EPR spectra and to measure variable-temperature magnetic susceptibility.

**Registry No.** $CoBr_2(DTBNO)_2$, 34923-18-7.

(17) Griffith, J. S. *Struct. Bonding (Berlin)* **1972**, *10*, 87.

(18) Scaringe, J.; Hodgson, D. J.; Hatfield, W. E. *Mol. Phys.* **1978**, *35*, 701.
(19) Banci, L.; Bencini, A.; Gatteschi, D. *Inorg. Chem.* **1983**, *22*, 2681.
(20) Bencini, A.; Benelli, C.; Gatteschi, D.; Zanchini, C. *Inorg. Chem.* **1979**, *18*, 2137.

Contribution from the Department of Chemistry, University of California, Riverside, California 92521, and School of Chemical Sciences, University of Illinois, Urbana, Illinois 61801

# Interaction of Dioxygen with Binuclear Nitride-Bridged Iron Porphyrins

DAVID F. BOCIAN,*[1a,b] ERIC W. FINDSEN,[1a] JOSEPH A. HOFMANN, JR.,[1a] G. ALAN SCHICK,[1a] DANIEL R. ENGLISH,[1c] DAVID N. HENDRICKSON,*[1c] and KENNETH S. SUSLICK*[1c]

*Received August 4, 1983*

An unusual interaction between $O_2$ and nitride-bridged iron porphyrin dimers in frozen polar glasses has been found. The EPR spectrum previously attributed to a pyridine monoadduct of ($\mu$-nitrido)bis[(5,10,15,20-tetraphenylporphinato)iron] is in fact due to an $O_2$ adduct of the dimeric porphyrin. Optical spectroscopy shows that the $O_2$/porphyrin interaction is weak. Mössbauer spectra demonstrate that the two iron ions are inequivalent in the adduct while EPR data indicate a less anisotropic g tensor and appreciably diminished $^{14}N$ and $^{57}Fe$ hyperfine coupling relative to the nonadducted species. $O_2$ titrations, as monitored by EPR, show that the adduct's stoichiometry is one $O_2$ per dimer. All these data are consistent with a weak axial interaction of $O_2$ with one side of the $\mu$-nitrido dimer.

## Introduction

The interaction of $O_2$ with metalloporphyrins has been of continued intense study. Several $O_2$ complexes of iron(II) porphyrins, analogous to those of myoglobin and hemoglobin, have been exhaustively examined.[2] Little has been reported, however, on the interaction of higher oxidation state iron porphyrin complexes with $O_2$. We describe here the complexation of $O_2$ to ($\mu$-nitrido)bis[(porphyrinato)iron] dimers in frozen polar glasses.

The nitride-bridged iron porphyrin dimer[3] $((TPP)Fe)_2N$ has been the subject of a number of recent experimental[4-9] and

(1) (a) University of California. (b) Alfred P. Sloan Foundation Fellow, 1982-1984. (c) University of Illinois.
(2) (a) Ho, C., Ed. "Hemoglobin and Oxygen Binding"; Elsevier: New York, 1983. (b) Collman, J. P.; Halbert, T. R.; Suslick, K. S. "Metal Ion Activation of Dioxygen"; Spiro, T. G., Ed.; Wiley: New York, 1980; pp 1-72. (c) Jones, R. D.; Summerville, D. A.; Basolo, F. *Chem. Rev.* **1979**, *79*, 139-178. (d) Traylor, T. G. "Bioorganic Chemistry"; van-Tamelen, E. E., Ed.; Academic Press: New York, 1978; Vol. IV, pp 437-468.

(3) Abbreviations: ($\mu$-nitrido)bis[(5,10,15,20-tetraphenylporphinato)iron], $((TPP)Fe)_2N$; ($\mu$-nitrido)bis[(2,3,7,8,12,13,17,18-octaethylporphinato)iron], $((OEP)Fe)_2N$; ($\mu$-nitrido)bis{[5,10,15,20-tetrakis-(3,4,5-trimethoxyphenyl)porphinato]iron}, $((TTMPP)Fe)_2N$; electron paramagnetic resonance, EPR; highest occupied molecular orbital, HOMO.
(4) (a) Summerville, D. A.; Cohen, I. A. *J. Am. Chem. Soc.* **1976**, *98*, 1747-1752. (b) Scheidt, W. R.; Summerville, D. A.; Cohen, I. A. *Ibid.* **1976**, *98*, 6623-6628.
(5) Kadish, K. M.; Bottomley, L. A.; Brace, J. G.; Winograd, N. *J. Am. Chem. Soc.* **1980**, *102*, 4341-4344.
(6) (a) Schick, G. A.; Bocian, D. F. *J. Am. Chem. Soc.* **1980**, *102*, 7982-7984. (b) *Ibid.* **1983**, *105*, 1830-1838.

0020-1669/84/1323-0800$01.50/0 

theoretical[10] studies. Unlike the analogous $\mu$-oxo dimer, which is diamagnetic at low temperatures due to antiferromagnetic exchange interactions between the two iron ions,[11] ((TPP)-Fe)$_2$N has a paramagnetic ground state, exhibiting a net spin $S = {}^1/_2$ over the temperature range 4–298 K,[4a,9] and is amenable to study by EPR spectroscopy.[4a,6a,8,9] The EPR spectrum of the complex in frozen carbon disulfide solution is characteristic of an axially symmetric spin system with a small **g** tensor anisotropy, $g_\perp \sim 2.15$ and $g_\parallel \sim 2.01$.[6a,9] In frozen toluene solutions, the **g** tensor is slightly rhombic with $g_x \sim 2.16$, $g_y \sim 2.15$, and $g_z \sim 2.01$.[8] (We will refer to the species exhibiting signals in the range $g \sim 2.15$–$2.16$ and $g \sim 2.01$ as I.) The EPR spectrum of I exhibits well-resolved $^{14}$N nuclear hyperfine splittings due to the interaction of the unpaired electron with the nucleus of the bridging nitrogen atom. The magnitudes of these splittings have been interpreted to indicate that the unpaired electron resides in a predominantly metal-centered molecular orbital containing a small amount of nitrido 2s character.[8,9] This interpretation is consistent with molecular orbital calculations that predict that the HOMO of ((TPP)Fe)$_2$N is 89% iron $d_{z^2}$ (44.5% on each iron) and 1.6% nitrido 2s in character.[10]

The addition of pyridine to toluene solutions of ((TPP)Fe)$_2$N has been reported to result in the appearance of new EPR signals at $g \sim 2.07$, $g \sim 2.01$, and $g \sim 2.00$, which exhibit no $^{14}$N nuclear hyperfine structure.[8] (We will refer to the species exhibiting these signals as II.) It was proposed that II is a pyridine monoadduct of ((TPP)Fe)$_2$N formed only at low temperatures (<200 K) and that it is characterized by a nearly axially symmetric **g** tensor ($g_\parallel \sim 2.07$ and $g_\perp \sim 2.00$–$2.01$) that results from the unpaired electron residing in a predominantly iron $d_{x^2-y^2}$ molecular orbital. More recently, however, it has been found that at high concentrations in carbon disulfide ((TPP)Fe)$_2$N exhibits EPR signals characteristic of a highly rhombic **g** tensor in addition to those of I.[9] The perturbations of the **g** tensor that occur at high concentrations suggest that the EPR signals observed from the complex are quite sensitive to the local environment in the frozen solvent–solute matrix.

In view of the sensitivity of the EPR spectra of this system to local environment, we have reexamined the spectroscopic and magnetic properties of ((TPP)Fe)$_2$N, as well as those of two other nitride-bridged iron porphyrin dimers,[3] ((TTMPP)Fe)$_2$N and ((OEP)Fe)$_2$N, under a variety of conditions. The results of EPR studies of the complexes in various solvents, both with and without the presence of dissolved gases, bases (e.g., pyridine), or water, are presented here in order to delineate the origin of the various EPR signals. In addition, species I and II have been further characterized via optical studies as well as magnetic Mössbauer and EPR investigations using $^{57}$Fe-enriched species. Finally, the electronic structures of I and II suggested by the experimental observations are discussed. A surprising result surfaces in this study: species II results from the 1:1 interaction of $O_2$ and ((TPP)Fe)$_2$N.

## Experimental Section

**A. Complex, Solvent, and Gas Preparation.** The compounds ((TPP)$^{56}$Fe)$_2$N, ((TPP)$^{57}$Fe)$_2$N, ((OEP)$^{56}$Fe)$_2$N, and ((TTMP)$^{56}$Fe)$_2$N were prepared as follows: Iron metal, purchased from New England Nuclear (95.15% enriched) or reduced from the respective oxide[12] ($^{57}Fe_2O_3$ was obtained from Oak Ridge National Laboratories, 90.24% enriched in $^{57}$Fe), was inserted into the porphyrins (Midcentury, Posen, IL) by using the acetic acid method.[12] The resulting iron porphyrin acetates were dissolved in freshly distilled benzene and vigorously stirred with hydrazoic acid to yield the iron porphyrin azides, which were converted to the nitrogen-bridged dimers.[3] The identities of the final products were confirmed by UV/vis and infrared spectroscopy.

The solvents toluene, chloroform, dichloromethane, and pyridine (Mallinckrodt, SpectAR grade) were purified and dried as follows: Toluene was washed with concentrated $H_2SO_4$, rinsed with water, dried over $CaCl_2$, and distilled from benzophenone ketyl under $N_2$. Chloroform was washed with water to remove the stabilizer, dried over $CaCl_2$, and distilled from $P_2O_5$ under $N_2$. Dichloromethane was washed with concentrated $H_2SO_4$ and rinsed first with $K_2CO_3$ solution and then water alone. This solvent was then dried over $CaCl_2$ and distilled from $P_2O_5$ under $N_2$. Pyridine was distilled from KOH under $N_2$. Absolute ethanol (Gold Shield, highest purity) was used without further purification.

$N_2$, $O_2$, Ar, He, and CO (Matheson) were all research purity (99.9%) or higher and were used without further purification. Mixtures of $O_2$ in $N_2$ were obtained as certified standards (Matheson) and used without further treatment. NO (Matheson, 99% purity) was passed through a KOH column prior to use to remove higher oxides of nitrogen.

*N*-(2,4-Dinitrophenyl)picrylhydrazyl (DPPH), 1,3,5-trinitrobenzene (TNB), 1,3,5-trinitroanisole (TNA), trinitromesitylene (TNM), 4-hydroxy-2,2,6,6-tetramethylpiperidinyl-1-oxy (TEMPOH), 2,4,5,7-tetranitro-9-fluorenone (TNF), tetracyanoethylene (TCNE), and tetracyanoquinone (TCNQ) were reagent grade and were used without further purification.

**B. EPR Spectroscopy.** The EPR spectra were recorded on a Bruker ER200D X-band spectrometer with a 12-in. magnet or a Varian E-9 X-band spectrometer. The temperature was controlled by either an Oxford Instruments ESR 9 liquid-He cryostat or a direct-immersion liquid-nitrogen Dewar. The concentrations of the samples used for the EPR studies were all 1 mg/mL unless otherwise noted. The solutions for EPR studies were prepared in a drybox under a $N_2$ atmosphere with use of porphyrin complexes dried for 40 h at 110 °C immediately prior to use. The samples were initially degassed directly in the EPR tube via 10–15 freeze–pump–thaw cycles. Pure gases or gas mixtures were introduced by bubbling through a syringe needle immersed in the sample that was contained in a glovebag under atmosphere of the particular gas.

**C. Optical Spectroscopy.** The optical spectra were recorded on a Cary 219D spectrophotometer on samples maintained at 77 K in a liquid-$N_2$ immersion Dewar. The sample concentrations, degassing procedures, and gas addition procedures were identical with those used for the EPR studies. Prior to recording a particular optical spectrum, the EPR spectrum of the sample was recorded directly from the flat 1-mm optical cuvette in order to confirm the presence of I and II. Initially, optical spectra were obtained for solvent mixtures containing primarily ethanol, which forms a high-quality optical glass at 77 K. It was found, however, that 100% conversion of I to II could not be effected in solvent mixtures containing more than 30–50% ethanol. Ultimately, the optical studies were conducted on 3:1 pyridine/ethanol mixtures that were found to form reasonably high-quality optical glasses and also allow a 100% conversion of I to II.

**D. Mössbauer Spectroscopy.** Mössbauer transmission spectra were collected by using a vertically positioned Ranger drive, a Reuter-Stokes Ar-$CO_2$ proportional counter, and a Canberra Series 30 analyzer operating in multiscaler mode. Synchronization was achieved by using the twice-integrated square wave signal (MSB) from the multichannel analyzer to generate the drive signal.

The source consisted of approximately 45 mCi of $^{57}$Co diffused in a rhodium matrix. Calibrations were made by using the known splittings of the metallic iron spectrum;[13] all isomer shifts are reported relative to room-temperature iron metal. In these calibrations, spectral line widths of approximately 0.27 mm/s were normally observed. The temperature of the absorber was monitored with either a GaAs or Si diode.

The spectral parameters (isomer shifts, quadrupole splittings, line widths, and relative areas) were obtained by a least-squares fitting to a sum of Lorentzian components. The fits were performed by using

(7) Kadish, K. M.; Rhodes, R. K.; Bottomley, L. A.; Goff, H. M. *Inorg. Chem.* **1981**, *20*, 3195–3200.
(8) Bottomley, L. A.; Garrett, B. B. *Inorg. Chem.* **1982**, *21*, 1260–1263.
(9) Schick, G. A.; Findsen, E. W.; Bocian, D. F. *Inorg. Chem.* **1982**, *21*, 2885–2887.
(10) Tatsumi, K.; Hoffmann, R. *J. Am. Chem. Soc.* **1981**, *103*, 3328–3341.
(11) Murray, K. S. *Coord. Chem. Rev.* **1974**, *12*, 1–35.
(12) Burke, J. M.; Kincaid, J. R.; Spiro, T. G. *J. Am. Chem. Soc.* **1978**, *100*, 6077–6083.
(13) Preston, R. S.; Hanna, S. S.; Heberle, J. *Phys. Rev.* **1962**, *128*, 2207–2218.

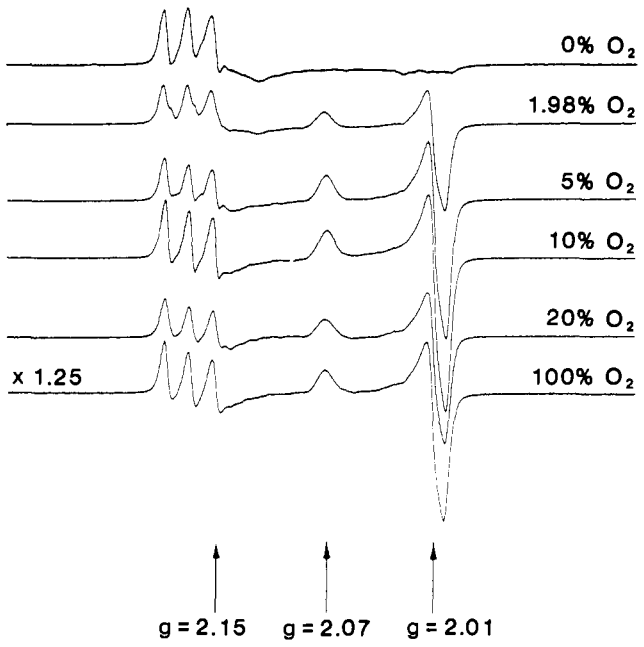


**Figure 1.** Effect of dissolved $O_2$ on the X-band EPR spectrum of $((TPP)Fe)_2N$ in dichloromethane at 77 K. The $O_2$ concentrations are given as the percentage of $O_2$ in an $O_2/N_2$ mixture. The spectra were recorded on 1 mg/mL samples with 2.8 mW of microwave power and 1.0 G of modulation amplitude.

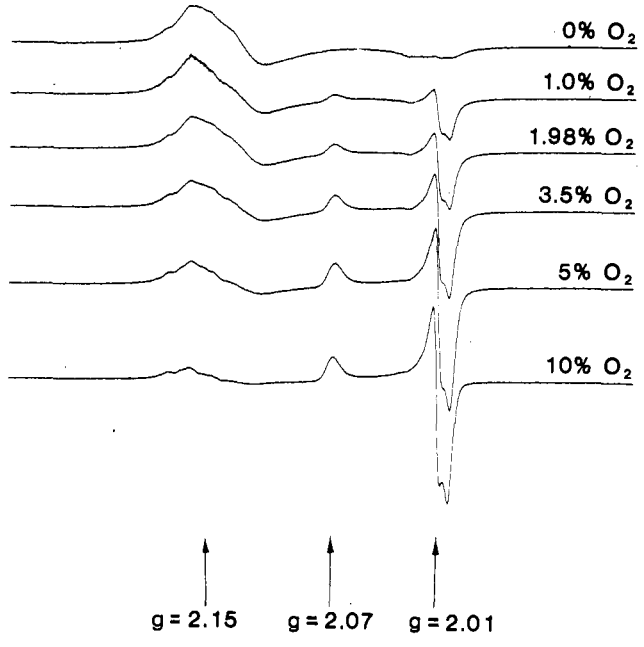


**Figure 2.** Effect of dissolved $O_2$ on the X-band EPR spectrum of $((TPP)Fe)_2N$ in pyridine at 77 K. The experimental conditions are identical with those given in the legend of Figure 1.

a modified Gauss–Newton iteration procedure. For spectra taken in the presence of an external magnetic field, the field was calculated by using the known sodium ferricyanide splittings.[14]

Samples for Mössbauer spectroscopy were prepared by dissolving the 95% $^{57}Fe$-enriched compound in the appropriate solvent or solvent mixture. Concentrations were 1 mg/mL, except for 2-MeTHF solutions, which were 0.4 mg/mL. One milliliter of solution was pipetted into the sample cell, and the sample was frozen in liquid nitrogen before placing it in the cryostat of the spectrometer. Examination of the solutions used for Mössbauer studies by EPR spectroscopy yielded spectra identical with those of separately prepared samples.

## Results and Discussion

**A. Influence of Environment on I and II. 1. Solvents, Inert Gases, and Water.** The low-temperature (77 K) EPR spectra of $((TPP)Fe)_2N$ in dichloromethane and pyridine solutions equilibrated at room temperature under pure $N_2$ are shown in the top traces of Figures 1 and 2, respectively. In both solvents signals are observed near $g \sim 2.15$ and $g \sim 2.01$, characteristic of I, although the $^{14}N$ nuclear hyperfine structure is only resolved in dichloromethane. The spectra obtained for toluene and chloroform and for various mixed toluene/pyridine solutions under pure $N_2$ also only exhibit EPR signals characteristic of I. The only difference in the various spectra is that the $^{14}N$ hyperfine structure is well resolved in toluene but becomes progressively more poorly resolved as pyridine is added and is not resolved at all in chloroform. The EPR spectra of $((TPP)Fe)_2N$ in rigorously degassed pure and mixed solvents, solvents equilibrated with Ar and He, and degassed and nondegassed solvents containing small amounts of water also failed to exhibit any trace of EPR signals attributable to II. Studies with $((OEP)Fe)_2N$ and $((TTMPP)Fe)_2N$ under the various conditions described above for $((TTP)Fe)_2N$ yielded similar results; namely, only EPR signals due to I were observed. Our result that only signals due to I are observed for mixed toluene/pyridine solutions of $((TPP)Fe)_2N$ is in *direct conflict* with that of an earlier EPR study by Bottomley and Garrett,[8] who reported that titration of toluene solutions of the complex with pyridine results in a monotonic decrease in the intensity of the signals due to I accompanied by the appearance of those due to II.

**2. Dissolved $O_2$.** The effects on the low-temperature EPR spectra of equilibrating the samples of $((TPP)Fe)_2N$ with $N_2/O_2$ mixtures are shown in the lower traces of Figures 1 and 2. The spectra were obtained for single samples of the complex that were successively reequilibrated with higher $O_2$ concentration mixtures by sparging. In the presence of $O_2$, EPR signals characteristic of II are observed for both dichloromethane and pyridine solutions and increase in intensity with increasing $O_2$ concentration. Reequilibration of the two samples with pure $N_2$ results in a complete regeneration of the EPR spectrum of I (top traces), while subsequent reintroduction of $O_2$ again generates signals due to II. Essentially identical results were obtained for $((OEP)Fe)_2N$ and $((TTMPP)Fe)_2N$ in dichloromethane and pyridine solutions and for all three complexes in the other pure solvents and solvent mixtures. *The only factor governing the appearance of the EPR signals due to II is the presence of dissolved $O_2$ in the solvent.*

Comparison of Figures 1 and 2 shows that the relative amounts of I and II observed at a particular $O_2$ concentration are sensitive to solvent choice. For example, under 10% $O_2$, EPR signals due to both species are clearly observed in dichloromethane solution of $((TPP)Fe)_2N$, while for pyridine solutions essentially only those due to II are present. Comparison of the EPR spectra of $((OEP)Fe)_2N$ and $((TTMPP)Fe)_2N$ (not shown) with those of $((TPP)Fe)_2N$ reveals that the amount of II observed with a particular solvent and $O_2$ concentration is also sensitive to the nature of the substituent groups on the complexes. Dichloromethane solutions of $((TPP)Fe)_2N$ under 100% $O_2$ exhibit signals indicative of substantial amounts of both species, while $((OEP)Fe)_2N$, with less bulky substituent groups, exhibits essentially only signals due to II and $((TTMPP)Fe)_2N$, with bulkier substituent groups, exhibits only signals due to I. Double integration of the EPR signals of $((TPP)Fe)_2N$ in pyridine at 4 and 77 K under 0% $O_2$, where only I is present, and under 20% $O_2$, where only II is present, indicates that the total number of spins of I and II are the same (±10%) at each temperature. Attempts were also made to quantitate the relative amounts of I and II for the complexes under conditions where signals

(14) Reiff, W. M. *Coord. Chem. Rev.* **1973**, *10*, 37–67.

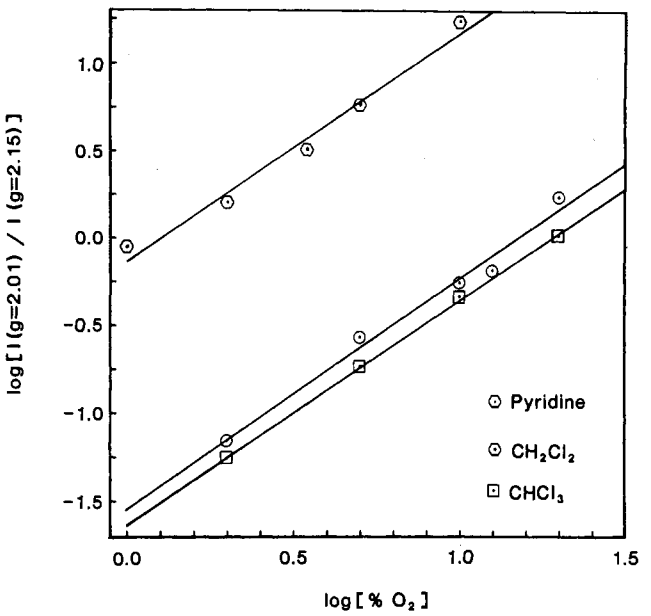


**Figure 3.** log–log plots of the ratio of the intensity of the $g = 2.01$ EPR signal of II and the $g = 2.15$ signal of I vs. the $O_2$ concentration for $((TPP)Fe)_2N$ in various solvents. The slopes of the lines are 1.3 ± 0.3.

from both species are observed; however, the severe overlap of the signals, along with the fact that the line widths are somewhat sensitive to the $O_2$ concentration, limits the accuracy of the measurement of the relative intensities. Nonetheless, log–log plots of the ratios of the intensities of the $g \sim 2.01$ signal of II and $g \sim 2.15$ signal of I (as measured by the peak heights) vs. $O_2$ concentration result in approximate straight lines with slopes in the range 1.0–1.3 ± 0.3. These plots are shown for $((TPP)Fe)_2N$ in Figure 3. The results suggest that there is an approximate 1:1 stoichiometry for the interaction between the nitride-bridged complexes and $O_2$.

The results of the $O_2$ titrations in toluene and pyridine solutions provide an explanation for the observations by Bottomley and Garrett[8] that pyridine apparently induces EPR signals due to II. We find that for all three of the nitride-bridged complexes studied no detectable amount of II is formed in toluene solutions, even under pure $O_2$. On the other hand, only small amounts of $O_2$ are necessary to produce a nearly quantitative conversion for I to II in pyridine solutions. Thus, titration of toluene solutions with incompletely degassed pyridine could result in an apparent sensitivity of the EPR spectrum to pyridine concentration. In this regard, we reexamined the EPR spectrum of $((TPP)Fe)_2N$ in mixed toluene/pyridine solutions prepared as described by Bottomley and Garrett by degassing the samples directly in the EPR tube via two or three freeze–pump–thaw cycles. Under these conditions EPR signals due to species II are still observed. Indeed, 15 freeze–pump–thaw cycles were not as effective in converting I to II as was bubbling with pure $N_2$ for several minutes.

**3. Dissolved CO and NO.** The observation that dissolved $O_2$ induces the conversion from I to II at low temperatures suggests that other diatomic gases that exhibit high affinities for monomeric iron porphyrins might also result in a species with EPR signals similar to those of II. In this connection, we examined the low-temperature EPR spectra of the nitride-bridged complexes in the presence of CO and NO. The EPR spectra in the presence of CO were found to exhibit only signals due to I. New EPR signals were observed in the presence of NO; however, these signals were not at all similar to those of II. Also, reequilibration of the samples under NO with $N_2$ failed to regenerate I. Subsequent studies of the species formed in the presence of NO revealed that the bridging ligand system was destroyed by reaction with NO.

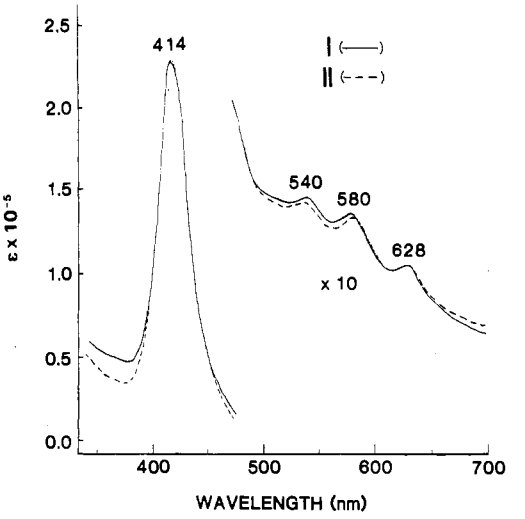


**Figure 4.** Comparison of the low-temperature (77 K) optical spectra of I and II in 3:1 pyridine/ethanol mixtures.

**4. Paramagnetic Species and π-Acid Complexing Agents.** The previous results indicate that $O_2$ has one or more properties that distinguish it from CO in this system. Two possibilities include the π-acid complexing ability and the paramagnetism of $O_2$.[15] Addition of the π-acids TNC, TNM, TNA, or TNF in up to 100-fold excess to a toluene solution of the dimer under an inert atmosphere produces no change in the spectrum. Addition of TCNQ or TCNE oxidizes the dimer to the monocation.[7,16] Addition of DPPH or TEMPOH results in EPR spectra in which the components are only attributable to combinations of the free radical and species I.

**B. Spectroscopic and Magnetic Properties of I and II.** The studies reported here indicate that the transformation from I to II is induced by the presence of dissolved $O_2$ in the solvent and that there is an approximate 1:1 interaction between $O_2$ and the nitride-bridged complexes. The question that remains to be answered is whether $O_2$ coordination to one iron atom of the dimer is occurring at low temperatures or whether the interaction is somewhat less specific. In attempts to elucidate the nature of the interaction of $O_2$ with the nitride-bridged complexes, we have examined the optical spectra of I and II along with the magnetic Mössbauer and EPR spectra of the two species using $^{57}Fe$-enriched $((TPP)Fe)_2N$.

**1. Optical Spectra.** Optical studies on a number of monomeric iron(II) porphyrins have shown that these complexes reversibly bind $O_2$ at low temperatures.[17–19] The studies have also shown that the amount of bound species formed is quite sensitive to the dielectric constant of the solvent, very little of the adduct being formed in low dielectric solvents such as toluene ($\epsilon \sim 2.38$) and substantial amounts being formed in high dielectric solvents such as dichloromethane ($\epsilon \sim 9.08$). These results are similar to those we report here for the relative amounts of I and II formed in toluene, dichloromethane, and pyridine ($\epsilon \sim 12.3$).

(15) (a) Slifkin, M. A. "Charge Transfer Interactions of Biomolecules"; Academic Press: New York, 1971. (b) Rosenberg, B.; Camiscoli, J. F. *J. Chem. Phys.* **1961**, *35*, 982–991. (c) Epstein, A.; Wildi, B. S. *Ibid.* **1960**, *32*, 324–329.
(16) English, D. R.; Hendrickson, D. N.; Suslick, K. S. *Inorg. Chem.* **1983**, *22*, 367–368.
(17) Ogoshi, H.; Watanabe, E.; Kincaid, J.; Nakamoto, K. *J. Am. Chem. Soc.* **1973**, *95*, 2845–2849.
(18) Baldwin, J. E.; Huff, J. *J. Am. Chem. Soc.* **1973**, *95*, 5757–5759.
(19) (a) Chang, C. K.; Traylor, T. G. *J. Am. Chem. Soc.* **1973**, *95*, 5810–5811. (b) *Ibid.* **1973**, *95*, 8475–8477. (c) *Ibid.* **1973**, *95*, 8477–8479.

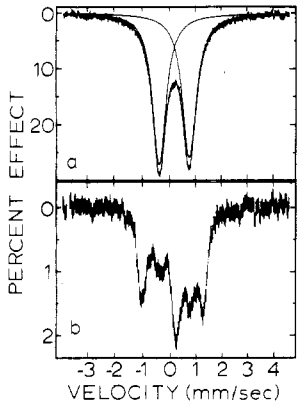


**Figure 5.** Mössbauer spectra of species I with zero external field: (a) solid sample at 7 K; (b) toluene solution at 12 K.

The formation of $O_2$ monoadducts of monomeric iron(II) porphyrins is generally accompanied by substantial changes in both the positions and intensities of the Soret and visible bands. Similar perturbations on the electronic structure could result upon monoaddition of $O_2$ to the nitride-bridged complexes, and these perturbations should be reflected in the optical spectra. The low-temperature (77 K) optical spectra of I and II for $((TPP)Fe)_2N$ are compared in Figure 4. As can be seen, the spectra of the two species are essentially superimposable. Similar results were obtained for the other complexes. These observations indicate that $O_2$ only perturbs the electronic structure of the complexes in a minor way.

**2. Mössbauer Spectra of $((TPP)^{57}Fe)_2N$.** The zero-field Mössbauer spectra for $((TPP)^{57}Fe)_2N$ in the solid state and in a 12 K toluene glass (1 mg/mL, prepared in air) are shown in Figure 5. A simple quadrupole-split doublet is observed for the solid sample; as can be seen in Figure 5, only one doublet is needed to fit this spectrum. On the other hand, in a 12 K toluene glass where only species I is present, the unpaired electron in $((TPP)^{57}Fe)_2N$ is relaxing slower than the inverse of the Mössbauer time scale and a magnetic pattern is seen (see lower tracing in Figure 5). This toluene glass sample was prepared three different times, and each time a magnetic pattern was obtained. The three spectra did vary somewhat in intensities of the individual lines; however, in each case the same spectral range and outer line positions were obtained. Apparently some small amount of solid precipitates when this glass is prepared, and this accounts for the slight variability in appearance of the spectrum. From the spectral range of this zero-field spectrum it is possible to calculate the internal magnetic field at the $^{57}Fe$ nucleus due to the single unpaired electron as $H_{int} = 88 \pm 10$ kG. This value is in keeping with the expectations for a Fermi contact of one unpaired electron interacting equivalently with the two $^{57}Fe$ nuclei.[20a,b] When the temperature of this toluene glass is

(20) (a) The value for the internal field was derived from computer simulations of the magnetic pattern.[20b] The estimate so made is accurate only to ~±10%. The value of 88 ± 10 kG agrees well with the iron hyperfine value obtained from simulation of the $^{57}Fe$ EPR spectrum. (b) Münck, E.; Groves, J. L.; Tumolillo, T. A.; Debrunner, P. G. *Comput. Phys. Commun.* **1973**, *5*, 225–238. (c) The EPR powder spectra of I were simulated as described by: Aasa, R.; Vänngård, T. *J. Magn. Reson.* **1975**, *19*, 308–315. Since the spin system is nearly axially symmetric, it was assumed that the principal axes of the hyperfine tensors of the $^{14}N$ and $^{57}Fe$ nuclei are coincident with those of the g tensor of the complex. The $g$ values and $^{14}N$ hyperfine coupling constants were taken from ref 8, and the line widths, Γ, were determined by simulating the spectrum of $((TPP)^{56}Fe)_2N$. The $^{57}Fe$ hyperfine coupling constants, $A_{^{57}Fe}$, were then determined by adjusting their values to fit the spectrum of $((TPP)^{57}Fe)_2N$ while leaving the values of $g$, $A_{^{14}N}$, and Γ unchanged. It should be noted that experiments and calculations of the present study indicate that the correct value for $g_y$ is 2.1471. The authors of ref 8 confirm that their X-band and EPR spectra are consistent with this value (Bottomley, L. A., private communication).

**Table I**

| medium[a] | temp, K | isomer shift(s),[b] mm/s | quadrupole splitting(s), mm/s | line half-widths,[c] mm/s |
|---|---|---|---|---|
| solid | 7 | 0.18 (2) | 1.12 (1) | 0.15, 0.15 |
| toluene | 100 | 0.17 (2) | 1.13 (1) | 0.21, 0.17 |
| toluene/ pyridine (3:1) | 10 | 0.15 (2), 0.15 (2) | 1.21 (2), 0.82 (2) | 0.14, 0.15, 0.17, 0.12 |
| pyridine/ ethanol (3:1) | 9 | 0.10 (2), 0.13 (2) | 1.45 (2), 1.03 (2) | 0.15, 0.20, 0.22, 0.13 |
| 2-MeTHF | 9 | 0.13 (2), 0.16 (2) | 1.11 (2), 0.83 (2) | 0.18, 0.20, 0.18, 0.18 |

[a] The toluene/pyridine and pyridine/ethanol solutions were 1 mg/mL in dimer concentration. The 2-MeTHF solution was 0.4 mg/mL in dimer concentration. [b] All isomer shifts are reported with respect to Fe metal at room temperature. For spectra where more than one doublet is present, the first value corresponds to the outer doublet while the second value corresponds to the inner doublet. [c] The line half-widths going from left to right correspond to the Lorentzian components passing from lower energy to higher energy.

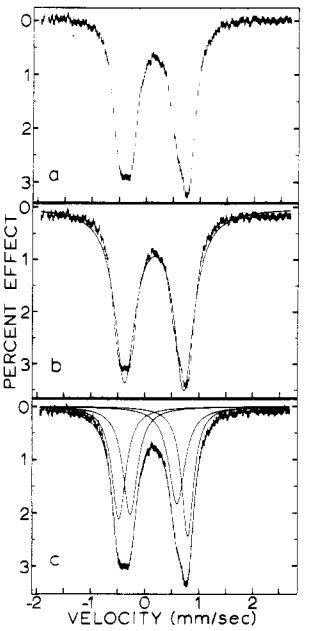


**Figure 6.** Mössbauer spectra of species II at 10 K in 3:1 toluene/pyridine: (a) experimental data in zero external field; (b) experimental data fit with a single doublet; (c) experimental data fit with two equal-area doublets.

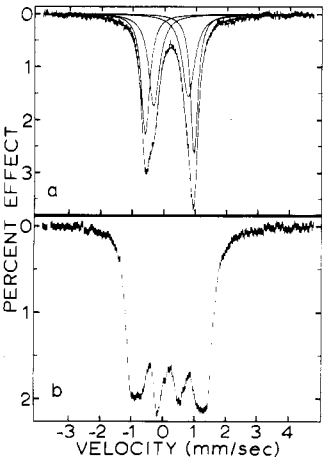


**Figure 7.** Mössbauer spectra of species II at 9 K in 3:1 pyridine/ethanol: (a) experimental data in zero external field, fit with two equal-area doublets; (b) experimental data with the application of a 36.5-kG external field.

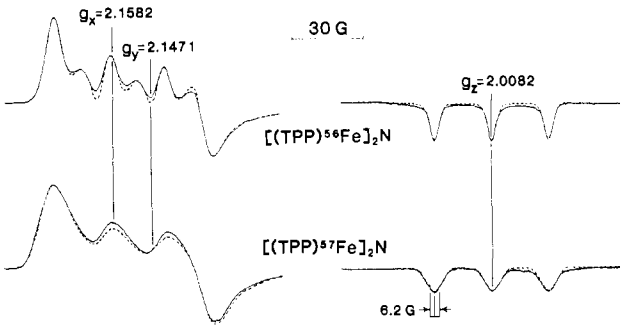


**Figure 8.** X-band EPR spectra of I for $((TPP)^{56}Fe)_2N$ and $((TPP)^{57}Fe)_2N$. The solid lines are the observed spectra recorded at a sample concentration of 1 mg/mL in toluene at 41 K with 2.8 mW of microwave power and 1.0 G of modulation amplitude. The recorder gain used in the $g = 2.01$ region is 0.63 times that used in the $g = 2.15$–$2.16$ region. The dashed lines represent spectra simulated by using the following parameters: $g_x = 2.1582$, $g_y = 2.1471$, $g_z = 2.0082$, $A^x_{^{14}N} = 67.27$ MHz, $A^y_{^{14}N} = 66.77$ MHz, $A^z_{^{14}N} = 66.16$ MHz, $A^x_{^{57}Fe} = -14.5$ MHz, $A^y_{^{57}Fe} = -14.5$ MHz, $A^z_{^{57}Fe} = 9.0$ MHz, $\Gamma_x = 3.6$ G, $\Gamma_y = 4.4$ G, and $\Gamma_z = 2.3$ G. The simulations represent the average of 8100 orientations in the magnetic field. Gaussian line shapes were used for the individual resonances in the powder spectra. The EPR spectrum of the $^{57}$Fe-substituted complex represents the statistically weighted average of the EPR traces calculated for the three expected $^{57}$Fe/$^{56}$Fe combinations on the basis of 90.24% Fe enrichment.

increased above 12 K, the electronic relaxation rate increases and the magnetic pattern changes into a simple quadrupole-split doublet with parameters similar to those obtained for the solid (see Table I).

In a glass formed from a more polar solvent, the Mössbauer characteristics of $((TPP)^{57}Fe)_2N$ differ markedly from those found for the toluene glass. Figures 6 and 7 illustrate this for toluene/pyridine (3:1) and pyridine/ethanol (3:1) glasses, respectively, at 10 K. Recall that under these conditions, only species II is present. Magnetic splitting of these Mössbauer spectra is not seen. Apparently, the proximity of the paramagnetic $O_2$ molecule has modified the electronic relaxation rates of the nitride-bridged complex. Another noteworthy characteristic of these spectra is that they cannot be fit by a single quadrupole-split doublet. This is clearly seen in comparing Figure 6b, in which a single doublet fit is attempted, with Figure 6c, in which two equal-area doublets are used. The fit does not improve appreciably by allowing the areas either of the two doublets or of the components of both doublets to vary independently during the least-squares minimization procedure. Thus, species II has nonequivalent iron sites, a fact that is evident even without the fitting process (note Figures 6a and 7a). Application of 36.5-kG external field produces a spectrum (Figure 7b) that is also indicative of more than one iron site (e.g., the most negative velocity band structure is clearly due to at least two features). These results are also found in other solvent systems except that the quadrupole splittings of the two doublets vary. The Mössbauer least-squares fitting parameters for $((TPP)^{57}Fe)_2N$ in different solvent systems are given in Table I. The Mössbauer parameters are more sensitive to the choice of solvent system than are the EPR spectra.

**3. EPR Spectra of $((TPP)^{57}Fe)_2N$.** The optical studies of I and II indicate that the interaction of $O_2$ with the nitride-bridged dimers results in no significant perturbation of the porphyrin electronic system. A knowledge of the $^{57}$Fe hyperfine coupling constants could shed some light on the electronic structure of species I and II and could demonstrate whether both iron ions are involved in the two EPR spectra. The low-temperature (41 K) X-band EPR spectra of I and II for $((TPP)^{57}Fe)_2N$ are compared with the respective $^{56}$Fe species in Figures 8 and 9. The EPR spectrum of $^{57}$Fe-enriched species I is quite different from that of the corresponding $^{56}$Fe complex. In the $g = 2.01$ region, each of the three $^{14}$N hyperfine components is broadened due to the hyperfine interaction from the two equivalent $^{57}$Fe nuclei. In the $g = 2.15$–$2.16$ region, the EPR signals do not exhibit any resolved $^{57}$Fe hyperfine splittings but are clearly broadened by the unresolved structure. The dashed line in Figure 8 represents the simulated spectrum due to $^{57}$Fe hyperfine (fitting parameters are given in the caption). The clear evidence for substantial $^{57}$Fe hyperfine splittings on the EPR signals of I can be contrasted to the observation that for II essentially no hyperfine splittings are apparent (Figure 9). The spectra of $^{57}$Fe and $^{56}$Fe II are so nearly identical that the $^{57}$Fe hyperfine splittings must be less than 1 G. Attempts were made to resolve the hyperfine splittings for both I and II by lowering the temperature, but no further narrowing of the EPR signals occurred as the temperature was lowered from 41 to 4 K. Computer simulation of the EPR powder spectra of species I did, however, result in the following values for the $^{57}$Fe hyperfine coupling constants: $|A_x| = |A_y| = 14.5$ MHz (4.8 G) and $|A_z| = 9.0$ MHz (3.1 G).[20c] The magnitude of these constants reflects that a large amount of the spin density in the complexes resides on the metal centers (see below).[21] Other experiments using enriched $^{17}O_2$ failed to show any detectable broadening of the EPR spectrum of II.

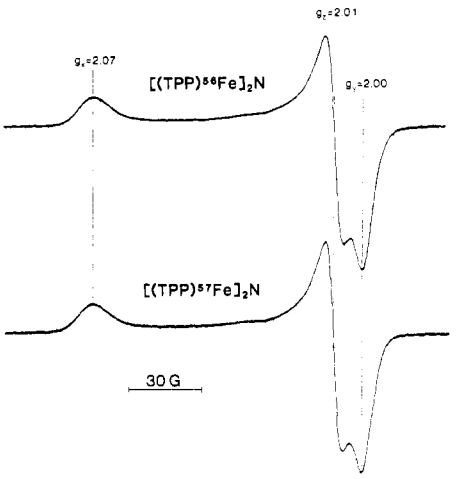


**Figure 9.** X-Band EPR spectra of II for $((TPP)^{56}Fe)_2N$ and $((TPP)^{57}Fe)_2N$ in pyridine at 41 K. The other experimental conditions are the same as those given in the legend of Figure 8.

Unfortunately the lack of any apparent $^{57}$Fe, $^{14}$N, or $^{17}$O hyperfine splittings for II precludes any quantitative determination of the spin distribution in the complex. However, for I a quantitative estimate of the spin density on the metal centers can be obtained by considering the following relationships for the hyperfine coupling constants of an electron in a $d_{z^2}$ orbital:[22]

$$A_\parallel = -K + {}^4/_7\beta^2 P - {}^1/_7(g_\perp - 2.0023)P$$

$$A_\perp = -K - {}^2/_7\beta^2 P + {}^{15}/_{14}(g_\perp - 2.0023)P$$

The first term in these equations is the isotropic Fermi contact contribution to the hyperfine coupling, and the second and third terms are the direct and indirect dipolar coupling contributions. The parameter $P$ is related to the anisotropic hyperfine coupling and has the value 98.6 MHz for an iron ion.[22] The parameter $\beta^2$ is the probability for the unpaired electron in the $d_{z^2}$ orbital. With use of the values $A_\perp = -14.5$ MHz and $A_\parallel = 9.0$ MHz,[23] $\beta^2$ (for each iron ion) is calculated

(21) (a) Münck, E. "The Porphyrins"; Dolphin, D. E., Ed.; Academic Press: New York, 1979; Vol. IV, pp 379–424. (b) Sams, J. R.; Tsin, T. B. *Ibid.* pp 425–478.

(22) McGarvey, B. R. *J. Phys. Chem.* **1967**, *71*, 51–67.

to be 49%. This value is consistent with the nearly isotropic $^{14}N$ hyperfine interaction observed for I, which suggests that only a small amount of the spin density resides on the bridging nitrogen atom.[8,9] The value 49% is also in excellent agreement with molecular orbital calculations,[10] which predict that an orbital characterized by 44.5% contribution from each iron ion contains the unpaired electron.

**C. Electronic Structure of I and II.** It is obviously difficult to specify on a molecular scale the nature of the weak interaction seen between $O_2$ and the $\mu$-nitrido iron porphyrin complex. At least four fundamentally different views of the molecular contact of these two species can be envisioned: (1) A magnetic exchange interaction between the triplet-state $O_2$ and doublet-state nitride complex results from a weak interaction of $O_2$ in an axial orientation with one iron atom. (2) The $O_2$ molecule in a singlet state interacts in an axial orientation with the nitride complex, leading only to a perturbation of the highest occupied molecular orbitals. (3) The $O_2$ molecule in either a triplet or singlet state is involved in a $\pi$-interaction with the porphyrin $\pi$-system. In this case a magnetic exchange interaction between triplet $O_2$ and the nitride dimer could be quite weak. (4) The electron is in large part transferred to the $O_2$ molecule, resulting in a $((TPP)Fe)_2N^+/O_2^-$ species.

In our opinion, view 1 seems the most plausible for the following reasons. An antiferromagnetic exchange interaction between triplet $O_2$ and the doublet iron porphyrin dimer would produce a doublet ground state and a quartet excited state. If the quartet state is significantly higher in energy than the doublet state, and therefore unpopulated, the EPR spectrum of the ground-state doublet would be seen. The EPR spectrum of species II is that expected for a simple doublet state. There are no features attributable to a quartet state. Also, the EPR intensity at 4 and 77 K is that expected for population of only the doublet state.

Magnetic exchange could also be invoked to explain the loss of superhyperfine from iron and nitrogen on passing from species I to species II. If the magnitude of the exchange interaction is greater than the energy of the hyperfine interaction, then the effective hyperfine interaction in the doublet ground state of the exchange-coupled $O_2$–$((TPP)Fe)_2N$ pair will be dramatically reduced. Obviously the magnetic exchange interaction does not need to be very large in order to have electron exchange that is rapid on the EPR time scale; an interaction where the exchange parameter $|J|$ is approximately 0.01 $cm^{-1}$ would be sufficient. Misalignment of **g** and **A** tensors in species II would also lead to a reduction of hyperfine splitting.

The second explanation invokes an interaction in which the $O_2$ is assumed to be functioning simply as a point-charge perturbation. With use of the molecular orbitals from the scheme proposed by Tatsumi and Hoffmann,[10] the $O_2$ molecule can be treated as an approaching point charge and differences in orbital energies required to produce the rhombic $g$ values for species II can be calculated. However, to produce the changes in the $g$ values that occur in passing from species I to species II, one must change the frontier orbital energies by approximately 5000 $cm^{-1}$. Such a large interaction would likely require an exchange interaction between triplet $O_2$ and the iron porphyrin doublet. The absence of such a magnetic exchange could be due to spin pairing to form $^1O_2$, caused by the interaction of $O_2$ with the dimer. The energy needed to do this, however, is on the order of 10000 $cm^{-1}$, which is too great to be available from stabilization of the porphyrin complex orbitals.

In the third view the $O_2$ molecule could interact with the porphyrin $\pi$-system through weak van der Waals forces. Several examples exist of physical adsorption of $O_2$ to porphyrin systems,[15,24] particularly at low temperatures, and $\pi$-molecular complex formation involving porphyrins is well-known. However, we have not been able to produce species II with a number of $\pi$-acid complexing agents in the place of $O_2$. Such an interaction, moreover, is likely to produce magnetic exchange as well, since it has been demonstrated that the porphyrin $\pi$-system and iron orbitals are strongly coupled[25] when the iron atom is out of the porphyrin plane as in $((TPP)Fe)_2N$.[4b]

Finally, in the fourth view, the $O_2$ adduct is best characterized as a diamagnetic $((TPP)Fe)_2N^+$ species coordinated to a superoxide ion. This configuration seems unlikely. The EPR spectrum of the $^{17}O_2$ adduct of the complex shows no evidence of broadening or structure due to $^{17}O$ hyperfine interactions. These would be expected if a substantial amount of the unpaired electron density is transferred to dioxygen.[26]

Regardless of the above details of the molecular interaction, the Mössbauer spectra show that the two iron ions of the binuclear complex are inequivalent in species II. This rules out a situation in which the $O_2$ molecule has slipped between the porphyrin planes, as interactions of this type would produce equivalent electric field gradient changes at the iron atoms. Thus, the Mössbauer spectra and the EPR titration experiment argue in favor of an interaction between one $O_2$ molecule and one side of the binuclear complex, perhaps involving a weak axial coordination to the iron.

Two remaining questions need to be addressed. First, why is species II not formed in toluene even under 1 atm of $O_2$? Possibly, this low dielectric solvent cannot stabilize the asymmetric charge distribution in the nitride–$O_2$ adduct. Second, why does CO not produce a species similar to II? This could be due to the greater polarizability of $O_2$ relative to CO. Or, perhaps CO does form such a weak complex, but because CO is not paramagnetic, there is no effect on the EPR signal.

## Conclusions

We have shown that $\mu$-nitrido iron porphyrin dimers interact with $O_2$ in polar frozen glass media. Optical spectroscopy shows that the interaction is weak. Mössbauer spectroscopic data show that the two iron atoms are inequivalent in the $O_2$ adduct. EPR data indicate that the **g** tensor becomes less anisotropic and the $^{14}N$ and $^{57}Fe$ hyperfine splittings are lost in passing from a polar frozen glass with no $O_2$ to one containing $O_2$. $O_2$ titrations monitored by EPR show that the ratio

(23) The signs of $A_x$ and $A_y \sim A_\perp$ can be inferred to be negative for the following reasons: The Fermi contact term and the direct dipolar coupling term give negative contributions to $A_\perp$ while the indirect dipolar coupling term gives a positive contribution.[22] The small anisotropy in the $g$ values of $((TPP)Fe)_2N$ dictates that the contribution of the indirect dipolar term is relatively small (15.9 MHz taking $g_\perp$ as the average $g_x$ and $g_y$). Since $|A_\perp|$ observed is 14.5 MHz, a positive value of $A_\perp$ would require that *both* $\beta^2$ and the Fermi contact term for the metal ions are near zero. This is unreasonable,[22] so $A_\perp$ must be negative. Unfortunately, the sign on $A_z \sim A_\parallel$ cannot be determined in the manner described above. The positive contribution of the direct dipolar coupling term makes either a positive or negative value for $A_\parallel$ reasonable. However, the positive value is more consistent with the nearly isotropic $^{14}N$ hyperfine interaction observed for $((TPP)Fe)_2N$, since a negative $A_\parallel$ results in a $\beta^2$ of only 29%. A value this low would require a substantial spin density on the bridging nitrogen atom, resulting in a significant anisotropy in the $^{14}N$ hyperfine interaction, which is not observed.

(24) Collman, J. P.; Brauman, J. I.; Suslick, K. S. *J. Am. Chem. Soc.* **1975**, *97*, 7185–7186. (b) Leal, O.; Anderson, D. L.; Bowman, R. G.; Basolo, F.; Burwell, R. L. *Ibid.* **1975**, *97*, 5125–5129.

(25) (a) Gans, P.; Marchon, J.-C.; Reed, C. A.; Regnard, J.-R. *Nouv. J. Chim.* **1981**, *5*, 201–202. (b) Scholz, W. F.; Reed, C. A.; Lee, Y. J.; Scheidt, W. R.; Lang, G. *J. Am. Chem. Soc.* **1982**, *104*, 6791–6793. (c) Buisson, G.; Deronzier, A.; Duée, E.; Gans, P.; Marchon, J.-C.; Regnard, J.-R. *Ibid.* **1982**, *104*, 6793–6794.

(26) (a) Melamud, E.; Silver, B. L.; Dori, Z. *J. Am. Chem. Soc.* **1974**, *96*, 4689–4690. (b) Tovrog, B. S.; Kitko, D. J.; Drago, R. S. *Ibid.* **1976**, *98*, 5144–5153.

of $O_2$ molecules to dimer molecules is 1:1 in the adduct. Thus, all of the results suggest that one $O_2$ molecule is axially interacting with one side of the dimer.

**Acknowledgment.** This work was supported in part by the donors of the Petroleum Research Fund, administered by the American Chemical Society (D.F.B.), the Cottrell Research Grants Program of the Research Corp. (D.F.B.), the Committee on Research, University of California, Riverside, CA (D.F.B.), and the National Institutes of Health (Grants GM30078 to D.F.B., HL13652 to D.N.H. and HL25934 to K.S.S.). We thank Peter Debrunner for useful comments.

**Registry No.** ((TPP)Fe)$_2$N, 59114-43-1; ((TTMPP)Fe)$_2$N, 88524-94-1; ((OEP)Fe)$_2$N, 88524-95-2; $O_2$, 7782-44-7; CO, 630-08-0; NO, 10102-43-9; DPPH, 88524-96-3; TNB, 99-35-4; TNA, 606-35-9; TNM, 602-96-0; TEMPOH, 2226-96-2; TNF, 746-53-2; TCNE, 670-54-2; TCNQ, 1518-16-7.

Contribution from the Dipartimento di Chimica Generale, Università di Pavia, 27100 Pavia, Italy

# Stepwise Incorporation of Copper(II) into a Double-Ring Octaaza Macrocycle and Consecutive Oxidation to the Trivalent State

LUIGI FABBRIZZI,* FABRIZIO FORLINI, ANGELO PEROTTI, and BARBARA SEGHI

*Received June 23, 1983*

The novel double-ring octaaza macrocycle **2** (*bisdioxocyclam*) has been prepared by the single-step aminolytic condensation of the appropriate tetraester and linear tetraamine in 1:2 molar ratio. The complexation of $Cu^{II}$ by **2** in aqueous solution has been investigated by potentiometric means. Monometallic and dimetallic complex species form according to the ligand:metal ratio. In general, incorporation of the $Cu^{II}$ ion into each tetraaza subunit promotes a simultaneous deprotonation of the two amido groups. log *k* values of complexation equilibria have been compared with those for the reference single-ring tetraaza macrocycle **1** (*dioxocyclam*). The [$Cu^{II}_2$(bisdioxocyclamato(4−))] complex undergoes a reversible oxidation to the dicopper(III) complex through two consecutive one-electron steps, whose electrode potentials are separated by 110 mV.

## Introduction

Whereas binuclear metal complexes have for several years been a classical topic of coordination chemistry, the number of investigations has increased dramatically more recently, due to the introduction of appropriate ligands, of the *macrocyclic* type, able to encapsulate two metal ions.[1] In fact, the closed nature of the ligand imparts both kinetic and thermodynamic stability to the dimetallic system, permitting the study of its solution behavior, an opportunity which has been rarely found with noncyclic ligand dinuclear complexes. In most of the reported systems the two metal ions, e.g. $Cu^{II}$, are accommodated in a large single-ring macrocycle[2] or in a three-dimensional molecular framework, formally derived from cryptands,[3] and face together. This constrictive situation may affect deeply electronic and magnetic properties and also mutually influence the redox activity of each metal center.

In contrast, we were interested in generating a situation in which the two proximate metal centers act as independently as possible. We thought that this goal could be achieved by preparing a ligand in which two small-ring macrocycles, able to accommodate a single metal ion, were linked together. A molecule of this type, in which two cyclam subunits are linked through a covalent bond, has been fortuitously obtained, in very small yield, as a side product in the template synthesis of cyclam.[4]

We have chosen as a subunit the tetraaza diamino–diamide macrocycle **1** (dioxocyclam) for the following reasons: (i) the

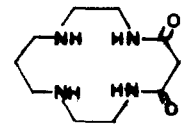

**1**

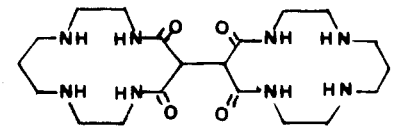

**2**

possibility exists to synthesize the dinucleating derivative **2** as a free molecule, according to an innovative single-step nontemplate reaction, with a satisfactory yield; (ii) the dioxocyclam unit can incorporate a $Cu^{II}$ ion, with simultaneous deprotonation of the two amido groups, according to a fast reversible equilibrium, which can therefore be investigated by conventional pH methods;[5] (iii) the $Cu^{II}$ ion, when incorporated in the dioxocyclamato(2−) unit, can be reversibly oxidized, at a moderately positive electrode potential, to give an authentic trivalent copper species that is stable in aqueous solution.[6]

We report here the synthesis of the novel double-ring macrocycle **2** (bisdioxocyclam), the study of the formation of mono- and dicopper(II) complexes of **2**, which involve several simultaneous pH-dependent equilibria, and the electrochemical investigation of the oxidation behavior of the above metal complexes. A preliminary report on the magnetic and redox properties of the dicopper(II) complex of bisdioxocyclam has appeared.[7]

## Experimental Section

**Synthesis of the Tetraaza Macrocycle (2). 1. 1,1,2,2-Ethanetetracarboxylate Tetraethyl Ester (3).** Preparation of **3** is based on the procedure reported by Bischoff and Rach.[8] A 0.2-mol amount of sodium is dissolved in 0.5 L of absolute ethanol in a three-neck

(1) See for example: Fenton, D. E.; Casellato, V.; Vigato, P. A.; Vidali, M. *Inorg. Chim. Acta* **1982**, *62*, 57.
(2) Drew, M. G. B.; Nelson, J.; Esho, F.; McKee, V.; Nelson, S. M. *J. Chem. Soc., Dalton Trans.* **1982**, 1837 and references therein.
(3) Lehn, J. M. *Pure Appl. Chem.* **1980**, *52*, 2441.
(4) Barefield, E. K.; Chueng, D.; Van Derveer, D. C.; Wagner, F. *J. Chem. Soc., Chem. Commun.* **1981**, 302.
(5) Kodama, M.; Kimura, E. *J. Chem. Soc., Dalton Trans.* **1979**, 325.
(6) Fabbrizzi, L.; Poggi, A. *J. Chem. Soc., Chem. Commun.* **1980**, 646.
(7) Buttafava, A.; Fabbrizzi, L.; Perotti, A.; Seghi, B. *J. Chem. Soc., Chem. Commun.* **1982**, 1166.
(8) Bischoff, C. A.; Rach, C. *Ber. Dtsch. Chem. Ges.* **1884**, *17*, 2781.

0020-1669/84/1323-0807$01.50/0 